Analysis of the HIV-1 Genomic RNA Dimerization Initiation Site Binding to Aminoglycoside Antibiotics Using Isothermal Titration Calorimetry

Serena Bernacchi, Eric Ennifar

Chapter 16

Analysis of the HIV-1 Genomic RNA Dimerization Initiation Site Binding to Aminoglycoside Antibiotics Using Isothermal Titration Calorimetry

Serena Bernacchi and Eric Ennifar

Abstract

Isothermal titration calorimetry (ITC) provides a sensitive, powerful, and accurate tool to suitably analyze the thermodynamic of RNA binding events. This approach does not require any modification or labeling of the system under analysis and is performed in solution. ITC is a very convenient technique that provides an accurate determination of binding parameters, as well as a complete thermodynamic profile of the molecular interactions. Here we show how this approach can be used to characterize the interactions between the dimerization initiation site (DIS) RNA localized within the HIV-1 viral genome and aminoglycoside antibiotics. Our ITC study showed that the 4,5-disubstituted 2-desoxystreptamine (2-DOS) aminoglycosides can bind the DIS with a nanomolar affinity and a high specificity.

Key words HIV-1, Viral RNA, Aminoglycosides, Dimerization initiation site, ITC, Thermodynamics, RNA–drug interaction

1 Introduction

Interaction of biological macromolecules either with each other or with small ligands constitutes the basis for molecular recognition. The development of the approaches providing a detailed understanding of these interactions at the molecular level is required to facilitate the design and development of drugs. In this frame, the isothermal titration calorimetry (ITC) is an equilibrium solution technique that directly *characterizes* all parameters regulating the molecular interactions [1–4]. In a typical experiment, aliquots of a titrant in the syringe are injected into the cell containing the sample. Upon each titration, the amount of heat either released or absorbed during the binding event is measured, leading in one single experiment the determination of all the binding parameters: the equilibrium dissociation constant (K_d), the reaction stoichiometry (n), the binding enthalpy (ΔH), the binding entropy (ΔS), and the Gibbs free energy change (ΔG). Moreover, the analysis at

Véronique Arluison and Frank Wien (eds.), *RNA Spectroscopy: Methods and Protocols*, Methods in Molecular Biology, vol. 2113, https://doi.org/10.1007/978-1-0716-0278-2_16, © Springer Science+Business Media, LLC, part of Springer Nature 2020

several temperatures gives also access to the heat capacity change (ΔCp). Importantly, thermodynamic analysis can give access to structural data and hence provides information on hydrogen bonding, hydrophobic interactions, and charge–charge interactions. A serious advantage of ITC over other alternative approaches is that ITC is a true solution technique which does not require any modification, labelling, or immobilization of any partner (truly label-free) and that there is no restriction in the molecular weight of the reagents or in the choice of the buffer composition. Since the measured enthalpy results not only from the heat of the binding events but also from other heat sources such as solvent effects and/or heat of dilution, one has to pay attention to prevent any buffer mismatch between the syringe and the sample cell (*see* **Note 1**). Importantly, the application field of ITC has been recently extended to kinetics, in addition to thermodynamics, by the development of kinITC [5–9]. This method leads to the determination of on- and off-rates close to those obtained by surface plasmon resonance [10, 11].

In this chapter, we provide a detailed protocol for the characterization of interactions between a fragment of viral RNA with aminoglycoside drugs. ITC is a well-adapted technique for the study of RNA/ligand interactions [12–17]. The RNA used in this chapter is a synthetic 23-nucleotide containing the HIV-1 genomic RNA dimerization initiation site (DIS). Dimerization of the genomic RNA is a crucial step of the HIV-1 retrovirus replication cycle. The DIS is a highly conserved stem–loop sequence located in the 5′-untranslated region of the viral genome which is essential for genome dimerization [18, 19]. A six-nucleotide palindromic sequence within the DIS promotes genome dimerization by forming a loop–loop complex (or kissing-loop complex) [20–23]. This initial kissing-loop complex is further stabilized in vitro into an extended duplex form by extension of interstrand Watson–Crick base pairs [24–28]. X-ray structures of the DIS as a loop–loop complex [29, 30] and as an extended duplex [31, 32] revealed striking resemblance with the bacterial 16 S ribosomal A site, which is the natural target of aminoglycoside antibiotics, thus opening the opportunity of targeting the HIV DIS using such compounds [33, 34]. In this frame, ITC analysis showed that the 4,5-disubstituted 2-desoxystreptamine (2-DOS) aminoglycosides, but not 4,6-disubstituted 2-DOS, can bind specifically DIS dimers. Binding parameters revealed that the specific interaction between aminoglycosides and DIS kissing loop is ensured by rings I, II, and III, while rings IV and V enhanced affinity through unspecific interaction with sugar phosphate backbone. The RNA determinants of this interaction were also investigated, and we could show that DIS hairpin monomer, as well as the HIV-1 subtype-B DIS sequence, is not specifically recognized by aminoglycosides. This exhaustive ITC analysis of the binding and thermodynamic

parameters contributed to solve crystal structures of the DIS kissing loop and extended duplex in complex with several 4,5-disubstituted 2-DOS aminoglycosides [35–39].

2 Materials

2.1 Instrumentation

1. iTC_{200}, PEAQ-ITC (MicroCal, Malvern Panalytical, Malvern, UK) or equivalent highly sensitive isothermal titration calorimeter (*see* **Note 2**).
2. Refrigerated centrifuge for a rotor adapted for 50-mL Falcon tubes.
3. Nanodrop ND-1000 Spectrophotometer (Thermo Fisher Scientific, Waltham, MA, USA) or equivalent.
4. Dry bath for 90 °C incubation of Eppendorf tubes.

2.2 Instrument Accessories

1. Hamilton glass loading syringes for calorimeter.
2. BD Luer-Lok 1-mL syringe.

2.3 Sample Preparation

1. 23-mer HIV-1 RNA (sequence 5′-CUGCUUGAAGUGCACACAGCAAG3′) was chemically synthetized at the 1 μmol scale and purified (>98%) as described previously [32].
2. Lividomycin, neomycin, or paromomycin sulfate, powder. These aminoglycosides were purchased from Sigma-Aldrich and used without further purification. Paromomycin is shown in this example.
3. Amicon Ultra-4 centrifugal filter unit 10,000 MWCO (Millipore, Billerica, MA, USA).
4. 10× ITC buffer: 250 mM potassium chloride, 20 mM magnesium chloride, 200 mM sodium cacodylate, pH 7.0 (*see* **Note 3**). Prepare 10 mL.
5. 1× ITC buffer: 150 mM potassium chloride, 2 mM magnesium chloride, 20 mM sodium cacodylate, pH 7.0. Prepare 10 mL.

3 Methods

3.1 Sample Preparation

For each experiment, 300 μL of RNA at 10–30 μM should be prepared.

1. RNA is aliquoted in 3 Eppendorf tubes, each tube containing 1 mL of RNA at 2 μM in pure water (*see* **Note 4**).
2. Heat RNA sample for 5 min at 90 °C and snap cool in water on ice at 0 °C for 10 min.

3. Add 111 μL of 10× ITC buffer in each Eppendorf tube.
4. RNA sample is concentrated to a final volume of ~300 μL using an Amicon Ultra-4 concentrator. Centrifuge for ~10 min at 4500 *g* at 10 °C (recommended speed in a swinging rotor). Higher temperature should be avoided in order to prevent the conversion from the loop–loop complex RNA to the extended duplex form [40].
5. Check the absorbance at 260 nm using a spectrophotometer (take a full spectrum and not a single value). Here a final concentration of 16.8 μM (in strand) is obtained.
6. Prepare 1 mL of aminoglycoside solution at a 400 μM concentration in 1× ITC buffer. This chapter shows an example with the paromomycin aminoglycoside. The optimal aminoglycoside concentration may be different for another compound.

3.2 Designing a Typical ITC Experiment

3.2.1 Experimental Considerations

During an ITC experiment, aliquots of ligand are injected into the sample cell. The interaction between the ligand and the molecule in the cell induces the release (exothermic interaction) or absorption (endothermic interaction) of heat which is directly measured by the calorimeter. The titration curve of kcal mol^{-1} vs. molar ratio (ligand/sample) is generated by the integration of each heat pulse with time and normalized for concentration. After the fitting of the resulting isotherm with a binding model, the affinity constant ($K_a = 1/K_d$), the stoichiometry (n), and the enthalpy of interaction (ΔH) are obtained. The Gibbs free energy change (ΔG) and the entropy change (ΔS) are deduced via the thermodynamic relationships:

$$\Delta G = -RT \ln K_a = RT \ln K_d$$

$$\Delta G = \Delta H - T\Delta S$$

The determination of the appropriate concentration of the component placed in the sample cell (MT) depends on the binding affinity, the stoichiometry, and the heat of binding ΔH. If the Wiseman coefficient ($c = n \cdot K_a \cdot MT$) calculated is in the 1–1000 range (preferably between 10 and 500) [3], a sigmoid is then obtained, and this allows the determination of the accurate binding constant and ΔH.

In general the required concentrations of sample in the cell are ranging from 5 to 100 μM. Typical concentration for the ligand in the injection syringe is normally 10–20 times higher (and even higher in the case of low Wiseman c value experiments [41–43]). These conditions will ensure that the cell sample will become saturated at the end of the titration experiment. Therefore, the sample requirement in order to perform an ITC experiment under ideal conditions (c~100) might be significant for biological low affinity systems. A crucial point to obtain high-quality ITC

experiments is to minimize the heat signal originated from mismatches between the solutions that are mixed (*see* **Note 1**). For this reason, it is imperative to prepare the two samples (from the syringe and the cell) rigorously in the same buffer.

3.2.2 Instrument Parameters

On iTC_{200} and PEAQ-ITC microcalorimeters, the glass titration syringe holds up to 40 μL. Typical injections are ranging from 0.25 to 2 μL. The number of injections per experiment should be set in order to saturate the RNA at the end of the titration (a final molar ratio of 3–5 is acceptable in most situations). The injection speed should be 0.5 μL s^{-1}. The spacing between the injections is a frequently overlooked parameter, leading to truncated peaks and erroneous data if a complete return to the baseline is not achieved. We have shown that the time required for equilibration is strongly dependent on the rate constants k_{on} and k_{off} of each system [9]. The spacing value can be set to 120 s by default on the iTC_{200}, but it might be increased to 240 s or even longer in some situations [5, 10]. The filter value on iTC_{200} instrument corresponds to the integration time that will be used to produce a single data point. Usually the filter period is set to 5 by default; however, setting 1 or 2 for a better sampling of each peak in view of performing a kinetic analysis of the thermodynamic data is also possible [6, 9]. This value is fixed to 1 on the PEAQ-ITC instrument and cannot be modified.

The feedback mode of the calorimeter setup should be set to "high gain," yielding the fastest response time. The "reference power" value corresponds to the baseline (in μCal s^{-1}) during the experiment. In the high gain mode, the instrument's reference power ranges from 0 to 12.25 μCal s^{-1} for the iTC_{200}. In most cases, the reference power can be fixed to 5 μCal s^{-1}. The stirring speed depends on the syringe geometry. It should be set to 1000 rpm for straight-bladed syringes on iTC_{200}, but this value can be reduced to 750 rpm for helical-bladed syringe available on both iTC_{200} and PEAQ-ITC (*see* **Note 5**).

Most experiments are performed between 4 and 37 °C (the instrument's theoretical operating range is 2–80 °C, but extremes are not usable in practice). The choice of the experiment temperature is often overlooked, while it might be crucial to optimize results in some situations. Indeed, most biomolecular interactions are characterized by a temperature dependence of the ΔH due to a negative heat capacity change (*see* **Note 6**). In addition, the van't Hoff relationship

$$\partial \ln K_d / \partial T = -\Delta H / (RT^2)$$

also shows that K_d is affected by temperature change. Changing the cell temperature is thus an easy way to play on the Wiseman c value.

3.3 Performing the ITC Experiment

Below is described the procedure for an iTC_{200} microcalorimeter. The experiment will be performed at 25 °C.

1. Fill the reference cell with ultrapure water using a 0.5-mL glass Hamilton syringe.
2. In the instrument controls tab, set the temperature at 25 °C in "Thermostat Control," and click "Set Jacket Temp."
3. Rinse the sample cell, two or three times, with 1× ITC buffer.
4. Warm up the RNA sample at 25 °C before loading in the sample cell.
5. Gently load the sample cell with 300 μL of RNA sample. The small excess should be removed. The final sample volume in the cell is ~280 μL. Care must be taken to avoid bubble formation in the sample cell.
6. To load the titration syringe, place a microcentrifuge tube with at least 70 μL of aminoglycoside sample at 400 μM. Place the syringe titration above the microcentrifuge tube in order that the tip of the syringe is immerged in ligand solution. Manual loading of the syringe is recommended since it is faster and safer than the semiautomatic procedure on the iTC_{200}, especially if the sample is viscous (i.e., with a buffer containing some glycerol or with highly concentrated protein). Connect the BD syringe to the titration syringe and load the sample manually by aspiration into the titration syringe (before aspiration, make sure that the plunger is in the open position). When the sample gets to the plunger, click "Close Fill Port" in the instrument controls tab; this will move the plunger tip down and block the fill port. Perform the "purge/refill" procedure to remove small air bubbles in the syringe. Unplug the BD syringe from the titration syringe.
7. Place the titration syringe into the sample cell.
8. Set the reference power to 5 μCal s^{-1}.
9. Set the initial delay to 100 s and the stirring speed to 1000 rpm or 750 rpm depending on the syringe geometry.
10. Set the number of injections to 28, the sample cell concentration to 0.0168 mM, and the concentration in the syringe to 0.4 mM. This ensures a final molar ratio of ~5, required in such RNA/ligand experiments.
11. Set the titration parameters (the number and volume of the injections as well as the spacing between two injections) in the "Injection Parameters" window into the "Advanced Experimental Design" tab. Set the first injection volume to 0.3 μL (*see* **Note 7**) and the next injection volume to 1.5 μL. Set the spacing between each injection to 150 s.

12. Press the "Start" button to begin the experiment. The experiment will start when both cells are thermostated at 25 °C.
13. A blank experiment should be also performed by injecting aminoglycoside into 1× ITC buffer without RNA, in order to subtract the heat of dilution from the reaction heat data.

3.4 ITC Data Analysis

Various software are available for ITC data processing: MicroCal Origin 7 (VP-ITC and iTC_{200} from MicroCal); NanoAnalyze (TA Instrument); AFFINImeter [8]; the NITPIC, SEDPHAT, and GUSSI package [44, 45], or the MicroCal PEAQ-ITC analysis software (Malvern PEAQ-ITC). ITC data analysis using the MicroCal Origin7 software was previously described in details in [46].

Here we will describe the procedure for data processing using the MicroCal PEAQ-ITC analysis software provided with the PEAQ-ITC instrument.

1. Open the software and select both the RNA–ligand titration and the blank experiment (use the "Ctrl" key to select both files). They are quickly processed and integrated by the software and integrated heats are displayed on the left tab (Fig. 1). Binding is detected for the RNA/ligand titration ("Binding" is displayed in green, Fig. 1a), whereas "No binding" is displayed in orange for the blank experiment (Fig. 1b).
2. On the right arrowhead of the blank experiment, change "No binding" for "Control" (now displayed in blue).
3. On the main "Fitting Model" window, change the fitting model from "One Set of Sites" to "Two Sets of Sites" (*see* **Note 8**).
4. On top of the main window, change from "Overview" to "Adjust Baseline." This tab allows to manually correct integration heat for each data point (Fig. 2).
5. The "Time Factor" parameter on the bottom of the window might be useful if the baseline is not stable (large oscillation of the baseline due to air-conditioning, for instance), but 5 is generally a good standard value.
6. The number of points per injection is set by default to 25, but this can be changed if necessary.
7. Baseline for the RNA/ligand experiment and the buffer/ligand control can be adjusted, if necessary. This is generally not required in good experimental conditions: well-maintained instrument, samples without aggregates and injections without bubbles, and no heat perturbation around the instrument.
8. On top of the main window, change from "Adjust Baseline" to "Assign Control." On "Control Parameter," change from "Fitted Offset" to "Single." The control experiment is then automatically selected. The "Line" Method is generally

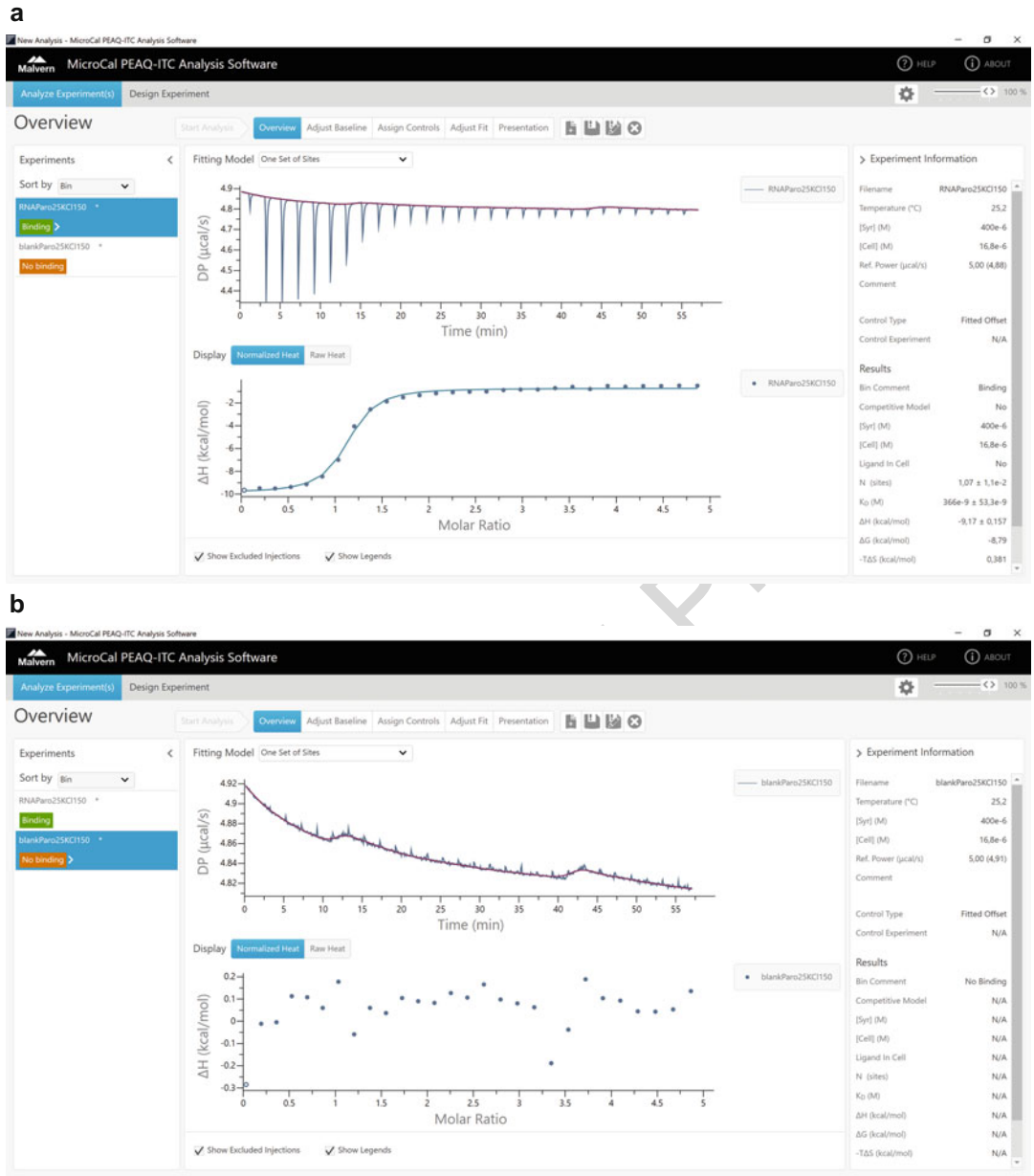

Fig. 1 Screenshot of the "Overview" tab after selection of the RNA/ligand (**a**) and the blank (**b**) experiment

preferable over the "Point-to-point" and "Mean" ones (Fig. 3). In the absence of control experiment, it is possible to use the heat of dilution from the last injections of the experiment, provided the RNA oversaturated with ligand. It is however highly recommended to perform a control experiment to obtain more accurate results.

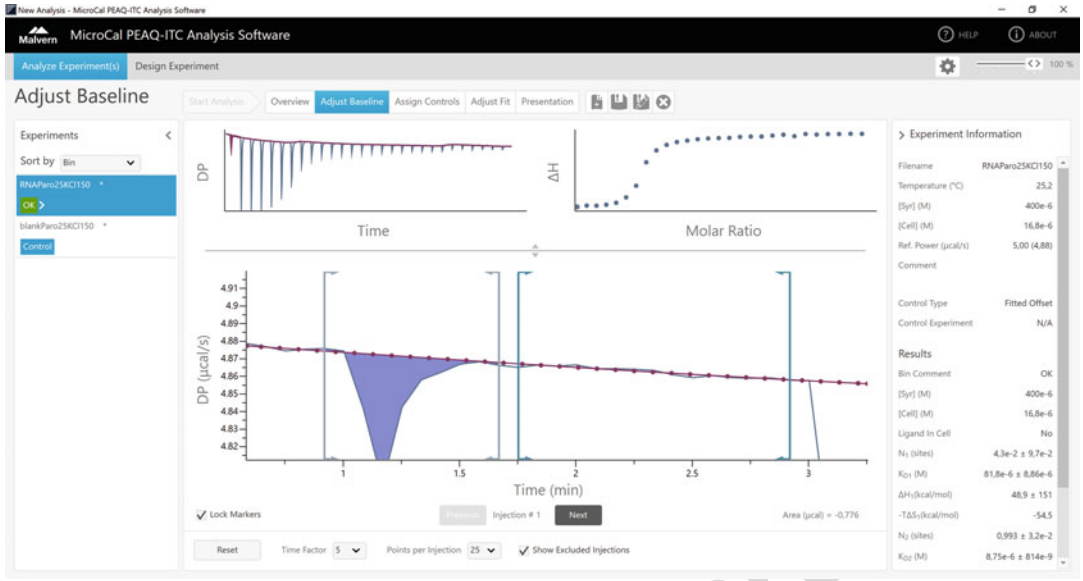

Fig. 2 Screenshot of the "Adjust Baseline" tab. The blue area corresponds to the integrated heat. It is possible to adjust the baseline by moving individually each point and the markers. Individual points can be excluded (or included) on the top-right part of the window

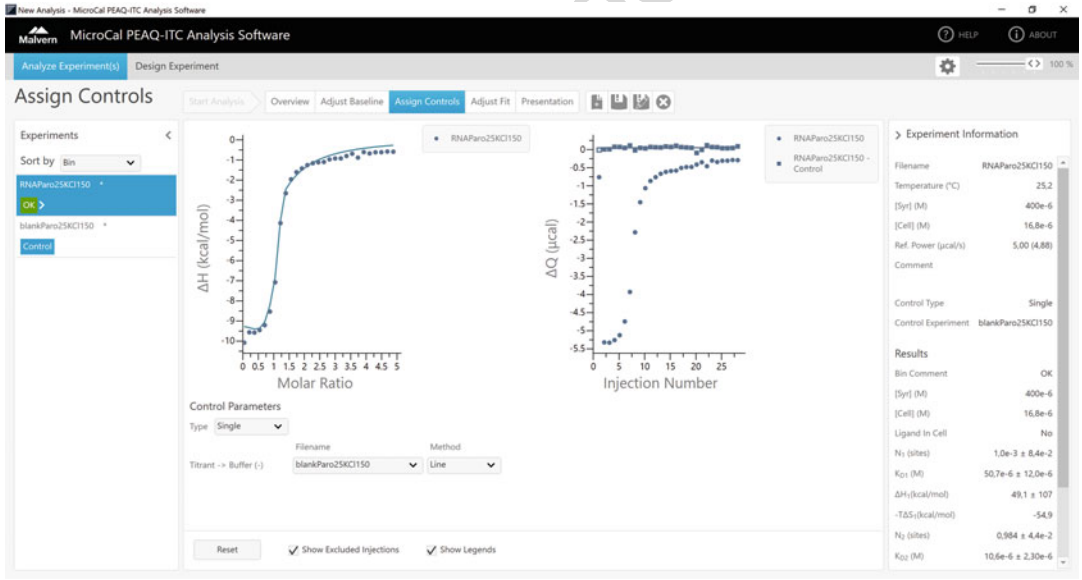

Fig. 3 Screenshot of the "Assign Control" tab. On the left part are shown the integrated heats for the experiment. On the right part are shown the integrated heats for the blank experiment and the corrected integrated heats for the experiment with RNA as well

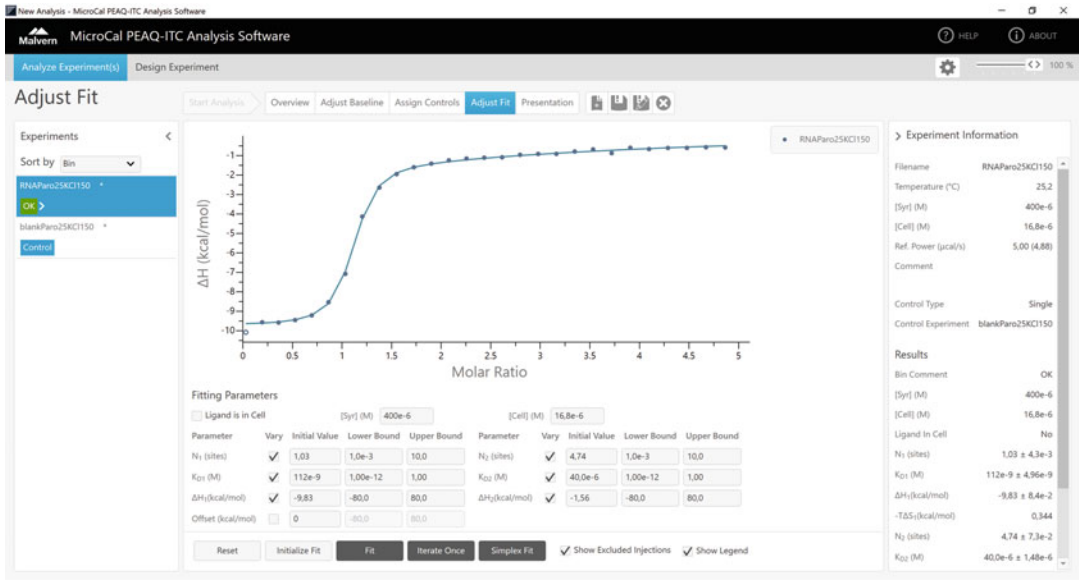

Fig. 4 Screenshot of the "Adjust Fit" tab

9. On top of the main window, change from "Assign Control" to "Adjust Fit." Fitted parameters can be adjusted here (Fig. 4). Here, N1 (which corresponds to the stoichiometry of the first class of binding sites) is very close to 1.0 (as expected since the RNA dimer binds two aminoglycoside ligands), showing that concentrations of the RNA and ligand were correctly estimated and that the RNA is properly folded. This binding site corresponds to the specific binding site and entails the highest affinity ($K_{d1} = 112$ nM, $\Delta H = -9.8$ kcal mol^{-1}). The stoichiometry of the second set of binding sites, N2, is relevant of unspecific binding due to electrostatic interactions with the lowest affinity ($K_{d2} = 40$ μM, $\Delta H = -1.6$ kcal mol^{-1}).
10. It is important to check errors on refined parameters! Indeed, in this model, the high correlation between the different fitted parameters could lead to multiple equivalent solutions.
11. On top of the main window, change from "Adjust Fit" to "Result Table." To visualize correlation between fitted parameters, click on "Show Errors" in the bottom of the window. The "dependency" value should be examined for all refined parameters (closer to 0 is better; closer to 1.0 is worst).
12. Select the "Final Figure" tab to display a publication quality figure (Fig. 5) which can be easily exported in various graphical formats.

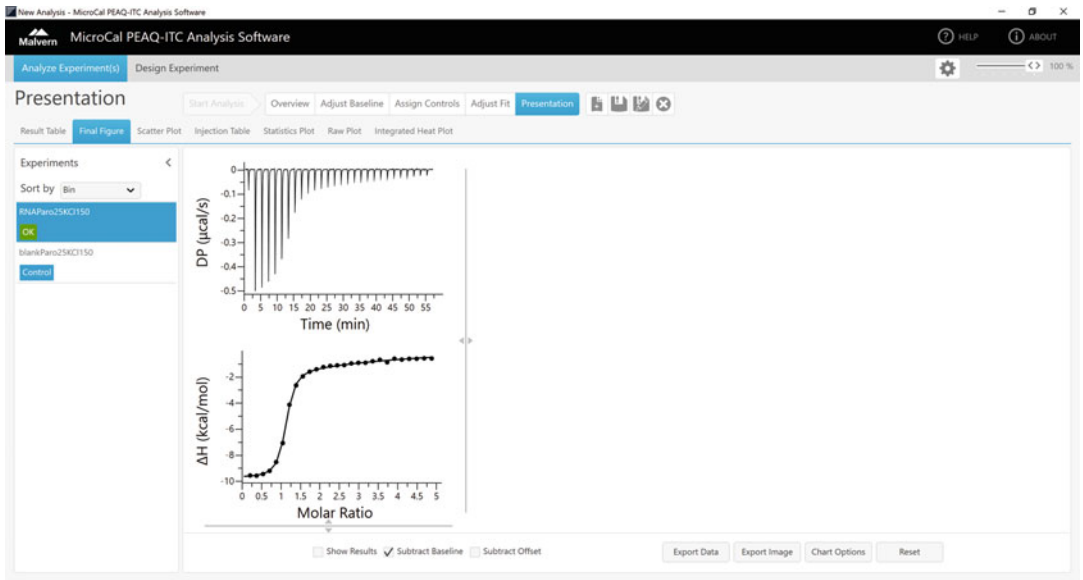

Fig. 5 Screenshot of the "Presentation" tab, showing the final figure ready to be exported for publication

4 Notes

1. Buffer mismatch is due to differences between the ligand and the sample solution, as well as any difference in pH, salt, glycerol concentration, buffer concentration, or additives. In order to minimize these differences, interactants must be prepared in identical buffers or dialyzed against the same buffer.
2. Since microcalorimeter (especially iTC_{200}) is very sensitive to temperature variations, it is highly recommended to place the instrument far away from any airflow, especially air-conditioning, and in a room exposed to minimal temperature changes (avoid heaters, large windows, or other instruments generating lots of heat such as freezers). The instrument should be regularly and meticulously cleaned.
3. Low-salt conditions were chosen at this temperature to prevent conversion of the loop–loop dimer into the extended duplex dimer [40].
4. RNA concentration at this step should be less than ~3 µM in order to prevent formation of extended duplex dimers as observed in [40].
5. Although the reduction of the stirring speed improves the baseline stability, it might introduce artifacts due to insufficient mixing of the injected ligand.

6. Heat capacity change is defined by the relationship:

$$\Delta C_p = (\delta \Delta H / \delta T)$$

The heat capacity change is generally negative and associated to a local folding following binding [47]. It is a valuable tool for optimizing the study of any binding event: for an exothermic reaction, ΔH will be more negative at 35 °C than 25 °C and, consequently, the signal will be increased at 35 °C. In some situations, no signal can be detected by ITC. This can result from athermal reactions (ΔH is null in the conditions of the experiment) where the interaction exists, but cannot be detected by ITC (an example is provided in [48]). In such situations, the change in temperature may allow the interaction to be observed due to the heat capacity change of the system.

7. A first small injection (0.3–0.5 μL) is performed at the beginning of the titration. It will be discarded during data analysis because it is generally affected by error due to sample dilution during the equilibration procedure and to the backlash of the screw mechanism of the syringe motor.

8. Since the aminoglycoside ligand is positively charged, the RNA/aminoglycoside interaction in this example is characterized by a highly specific interaction coexisting with unspecific interactions due to electrostatic interactions. These unspecific interactions can be strongly reduced by increasing salt concentrations (the specific interactionis also reduced, however). This situation holds true for most of RNA/ligand interactions.

References

1. Leavitt S, Freire E (2001) Direct measurement of protein binding energetics by isothermal titration calorimetry. Curr Opin Struct Biol 11:560–566
2. Privalov PL, Dragan AI (2007) Microcalorimetry of biological macromolecules. Biophys Chem 126:16–24
3. Velazquez Campoy A, Freire E (2005) ITC in the post-genomic era...? Priceless. Biophys Chem 115:115–124
4. Wiseman T, Williston S, Brandts JF, Lin LN (1989) Rapid measurement of binding constants and heats of binding using a new titration calorimeter. Anal Biochem 179:131–137
5. Bec G, Meyer B, Gerard MA, Steger J, Fauster K, Wolff P, Burnouf D, Micura R, Dumas P, Ennifar E (2013) Thermodynamics of HIV-1 reverse transcriptase in action elucidates the mechanism of action of non-nucleoside inhibitors. J Am Chem Soc 135:9743–9752
6. Dumas P, Ennifar E, Da Veiga C, Bec G, Palau W, Di Primo C, Pineiro A, Sabin J, Munoz E, Rial J (2016) Extending ITC to kinetics with kinITC. Methods Enzymol 567:157–180
7. Munoz E, Sabin J, Rial J, Perez D, Ennifar E, Dumas P, Pineiro A (2019) Thermodynamic and kinetic analysis of isothermal titration calorimetry experiments by using KinITC in AFFINImeter. Methods Mol Biol 1964:225–239
8. Pineiro A, Munoz E, Sabin J, Costas M, Bastos M, Velazquez-Campoy A, Garrido PF, Dumas P, Ennifar E, Garcia-Rio L, Rial J, Perez D, Fraga P, Rodriguez A, Cotelo C (2019) AFFINImeter: a software to analyze molecular recognition processes from experimental data. Anal Biochem 577:117–134
9. Burnouf D, Ennifar E, Guedich S, Puffer B, Hoffmann G, Bec G, Disdier F, Baltzinger M, Dumas P (2012) kinITC: a new method for obtaining joint thermodynamic and kinetic

data by isothermal titration calorimetry. J Am Chem Soc 134:559–565

10. Guedich S, Puffer-Enders B, Baltzinger M, Hoffmann G, Da Veiga C, Jossinet F, Thore S, Bec G, Ennifar E, Burnouf D, Dumas P (2016) Quantitative and predictive model of kinetic regulation by E. coli TPP riboswitches. RNA Biol 13:373–390
11. Zihlmann P, Silbermann M, Sharpe T, Jiang X, Muhlethaler T, Jakob RP, Rabbani S, Sager CP, Frei P, Pang L, Maier T, Ernst B (2018) KinITC-one method supports both thermodynamic and kinetic SARs as exemplified on FimH antagonists. Chemistry 24:13049–13057
12. Barbieri CM, Srinivasan AR, Pilch DS (2004) Deciphering the origins of observed heat capacity changes for aminoglycoside binding to prokaryotic and eukaryotic ribosomal RNA a-sites: a calorimetric, computational, and osmotic stress study. J Am Chem Soc 126:14380–14388
13. Feig AL (2007) Applications of isothermal titration calorimetry in RNA biochemistry and biophysics. Biopolymers 87:293–301
14. Feig AL (2009) Studying RNA-RNA and RNA-protein interactions by isothermal titration calorimetry. Methods Enzymol 468:409–422
15. Kaul M, Pilch DS (2002) Thermodynamics of aminoglycoside-rRNA recognition: the binding of neomycin-class aminoglycosides to the A site of 16S rRNA. Biochemistry 41:7695–7706
16. Pilch DS, Kaul M, Barbieri CM, Kerrigan JE (2003) Thermodynamics of aminoglycoside-rRNA recognition. Biopolymers 70:58–79
17. Salim NN, Feig AL (2009) Isothermal titration calorimetry of RNA. Methods 47:198–205
18. Haddrick M, Lear AL, Cann AJ, Heaphy S (1996) Evidence that a kissing loop structure facilitates genomic RNA dimerisation in HIV-1. J Mol Biol 259:58–68
19. Paillart J-C, Berthoux L, Ottmann M, Darlix J-L, Marquet R, Ehresmann C, Ehresmann B (1996) A dual role of the dimerization initiation site of HIV-1 in genomic RNA packaging and proviral DNA synthesis. J Virol 70:8348–8354
20. Laughrea M, Jetté L (1994) A 19-nucleotide sequence upstream of the 5′ major splice donor site is part of the dimerization domain of human immunodeficiency virus 1 genomic RNA. Biochemistry 33:13464–13474
21. Muriaux D, Girard PM, Bonnet-Mathonière B, Paoletti J (1995) Dimerization of HIV-1lai RNA at low ionic strength. J Biol Chem 270:8209–8216
22. Paillart JC, Skripkin E, Ehresmann B, Ehresmann C, Marquet R (1996) A loop-loop "kissing" complex is the essential part of the dimer linkage of genomic HIV-1 RNA. Proc Natl Acad Sci U S A 93:5572–5577
23. Skripkin E, Paillart JC, Marquet R, Ehresmann B, Ehresmann C (1994) Identification of the primary site of the human immunodeficiency virus type I RNA dimerization *in vitro*. Proc Natl Acad Sci U S A 91:4945–4949
24. Laughrea M, Jetté L (1996) Kissing-loop model of HIV-1 genome dimerization: HIV-1 RNA can assume alternative dimeric forms, and all sequences upstream or downstream of hairpin 248-271 are dispensable for dimer formation. Biochemistry 35:1589–1598
25. Muriaux D, Fossé P, Paoletti J (1996) A kissing complex together with a stable dimer is involved in the HIV-1_{Lai} RNA dimerization process *in vitro*. Biochemistry 35:5075–5082
26. Rist MJ, Marino JP (2002) Mechanism of nucleocapsid protein catalyzed structural isomerization of the dimerization initiation site of HIV-1. Biochemistry 41:14762–14770
27. Takahashi KI, Baba S, Chattopadhyay P, Koyanagi Y, Yamamoto N, Takaku H, Kawai G (2000) Structural requirement for the two-step dimerization of human immunodeficiency virus type 1 genome. RNA 6:96–102
28. Takahashi KI, Baba S, Koyanagi Y, Yamamoto N, Takaku H, Kawai G (2001) Two basic regions of NCp7 are sufficient for conformational conversion of HIV-1 dimerization initiation site from kissing-loop dimer to extended-duplex dimer. J Biol Chem 276:31274–31278
29. Ennifar E, Dumas P (2006) Polymorphism of bulged-out residues in HIV-1 RNA DIS kissing complex and structure comparison with solution studies. J Mol Biol 356:771–782
30. Ennifar E, Walter P, Ehresmann B, Ehresmann C, Dumas P (2001) Crystal structures of coaxially stacked kissing complexes of the HIV-1 RNA dimerization initiation site. Nat Struct Biol 8:1064–1068
31. Ennifar E, Walter P, Dumas P (2010) Cation-dependent cleavage of the duplex form of the subtype-B HIV-1 RNA dimerization initiation site. Nucleic Acids Res 38:5807–5816
32. Ennifar E, Yusupov M, Walter P, Marquet R, Ehresmann B, Ehresmann C, Dumas P (1999) The crystal structure of the dimerization initiation site of genomic HIV-1 RNA reveals an

extended duplex with two adenine bulges. Structure 7:1439–1449

33. Ennifar E, Paillart JC, Marquet R, Ehresmann B, Ehresmann C, Dumas P, Walter P (2003) HIV-1 RNA dimerization initiation site is structurally similar to the ribosomal A site and binds aminoglycoside antibiotics. J Biol Chem 278:2723–2730
34. Bernacchi S, Freisz S, Maechling C, Spiess B, Marquet R, Dumas P, Ennifar E (2007) Aminoglycoside binding to the HIV-1 RNA dimerization initiation site: thermodynamics and effect on the kissing-loop to duplex conversion. Nucleic Acids Res 35:7128
35. Ennifar E, Aslam MW, Strasser P, Hoffmann G, Dumas P, van Delft FL (2013) Structure-guided discovery of a novel aminoglycoside conjugate targeting HIV-1 RNA viral genome. ACS Chem Biol 8:2509–2517
36. Ennifar E, Paillart JC, Bernacchi S, Walter P, Pale P, Decout JL, Marquet R, Dumas P (2007) A structure-based approach for targeting the HIV-1 genomic RNA dimerization initiation site. Biochimie 89:1195–1203
37. Ennifar E, Paillart JC, Bodlenner A, Walter P, Weibel JM, Aubertin AM, Pale P, Dumas P, Marquet R (2006) Targeting the dimerization initiation site of HIV-1 RNA with aminoglycosides: from crystal to cell. Nucleic Acids Res 34:2328–2339
38. Freisz S, Lang K, Micura R, Dumas P, Ennifar E (2008) Binding of aminoglycoside antibiotics to the duplex form of the HIV-1 genomic RNA dimerization initiation site. Angew Chem Int Ed Engl 47:4110–4113
39. Bodlenner A, Alix A, Weibel JM, Pale P, Ennifar E, Paillart JC, Walter P, Marquet R, Dumas P (2007) Synthesis of a neamine dimer targeting the dimerization initiation site of HIV-1 RNA. Org Lett 9:4415–4418
40. Bernacchi S, Ennifar E, Toth K, Walter P, Langowski J, Dumas P (2005) Mechanism of hairpin-duplex conversion for the HIV-1 dimerization initiation site. J Biol Chem 280:40112–40121
41. Tellinghuisen J (2008) Isothermal titration calorimetry at very low c. Anal Biochem 373:395–397
42. Tellinghuisen J (2016) Analysis of multitemperature isothermal titration calorimetry data at very low c: global beats van't Hoff. Anal Biochem 513:43–46
43. Turnbull WB, Daranas AH (2003) On the value of c: can low affinity systems be studied by isothermal titration calorimetry? J Am Chem Soc 125:14859–14866
44. Brautigam CA, Zhao H, Vargas C, Keller S, Schuck P (2016) Integration and global analysis of isothermal titration calorimetry data for studying macromolecular interactions. Nat Protoc 11:882–894
45. Keller S, Vargas C, Zhao H, Piszczek G, Brautigam CA, Schuck P (2012) High-precision isothermal titration calorimetry with automated peak-shape analysis. Anal Chem 84:5066–5073
46. Da Veiga C, Mezher J, Dumas P, Ennifar E (2016) Isothermal titration calorimetry: assisted crystallization of RNA-ligand complexes. Methods Mol Biol 1320:127–143
47. Spolar RS, Record MT Jr (1994) Coupling of local folding to site-specific binding of proteins to DNA. Science 263:777–784
48. Ramirez J, Recht R, Charbonnier S, Ennifar E, Atkinson RA, Trave G, Nomine Y, Kieffer B (2015) Disorder-to-order transition of MAGI-1 PDZ1 C-terminal extension upon peptide binding: thermodynamic and dynamic insights. Biochemistry 54:1327–1337